Bull. Chem. Soc. Jpn. Vol. 80, No. 8, 1563–1572 (2007)

Selected Paper

Heterometal Assembly in Dendritic Polyphenylazomethines

Kensaku Takanashi, Atsunobu Fujii, Reina Nakajima, Hiroshi Chiba, Masayoshi Higuchi, Yasuaki Einaga, and Kimihisa Yamamoto*

Department of Chemistry, Faculty of Science and Technology, Keio University, 3-14-1 Hiyoshi, Kouhoku-ku, Yokohama 223-8522

Received January 12, 2007; E-mail: yamamoto@chem.keio.ac.jp

Fine-controlled metal–organic hybridization is strongly desired for advanced nano-materials. Dendrimers are highly branched organic macromolecules with successive layers or "generations" of branch units surrounding a central core. Metal–organic hybrid versions have also been produced by trapping metal ions or metal clusters within the voids of dendrimers. Here, we report a technique to form a dendritic organic structure, which includes various metals, with fine control over the number and location of the metal salts through a radial stepwise complexation. $FeCl_3$, $GaCl_3$, VCl_3, and $SnCl_2$ were decorated on a phenylazomethine dendrimer with 4th generations at the first, second, third, and forth layers, respectively. These stepwise complexation and heterometal assembling were also supported by TEM observation, ^{57}Fe Mössbauer spectroscopy, XPS measurement, and NMR spectroscopy.

Recently, with the development of nanotechnology, fine-controlled metal–organic hybridization is strongly desired for advanced nano-materials. For instance, in the research of metal complexes, a catalyst system in which the metal is precisely arranged has been examined. One of the ultimate shapes for this system is a protein in which the number and location of metal ions are precisely controlled.[1–3]

The use of dendrimers[4] has attracted much attention for catalyst[5] and cluster synthesis.[6] Dendrimers have a single molecular weight and three-dimensional spreading structure, in which the density of the branches increases radially outward. Due to these structural properties,[4,7] dendrimers are expected to be useful as templates for the generation of clusters with narrow dispersity or fine-controlled macromolecular complexes.

The present authors have reported the stepwise complexation of dendritic polyphenylazomethine (DPA, Fig. 1) with Sn[8,9] and Fe[10,11] ions by exploiting the basicity gradient of the constituent imines. It has been demonstrated that, through stepwise radial complexation, it is possible to control the position of complexation and the order of release in the molecule[9] and the complexation order can be controlled by the substituents chosen for the core phenyl.[12]

Based on this stepwise complexation, several kinds of metal ions might be decorated on the molecules with their number and location precisely controlled. The precise control of several kinds of metals on the molecules is expected to have novel effects on the catalysis system and synthesis of the heterometal clusters.

We now report the stepwise complexation of DPA with $GaCl_3$ and VCl_3. Further, we demonstrate the selective layering of 2–4 kinds of metals on DPA.

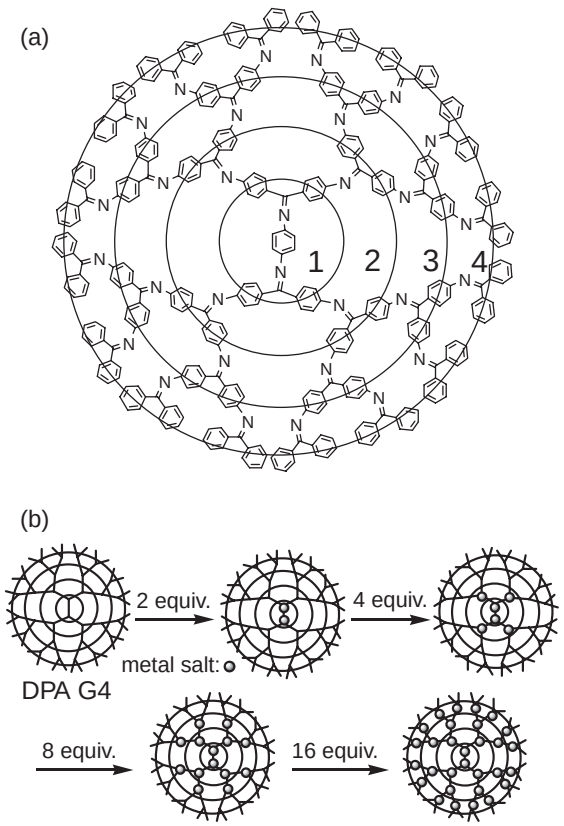

Fig. 1. (a) Dendritic polyphenylazomethine G4 (DPA G4). (b) Schematic representation of stepwise complexation of DPA G4 with metal salts.

Results and Discussion

Stepwise Complexation of DPA with $GaCl_3$ and VCl_3. The stepwise complexation of DPA with $SnCl_2$ and $FeCl_3$ was confirmed based on the shift in the isosbestic points during UV–vis titration and layer-selective reduction.[8–10] In the investigation of other metal salts that complexed with DPAs, $GaCl_3$, and VCl_3 were identified for further analysis.

The titrations of DPA G4 with metals were investigated by

Published on the web August 10, 2007; doi:10.1246/bcsj.80.1563

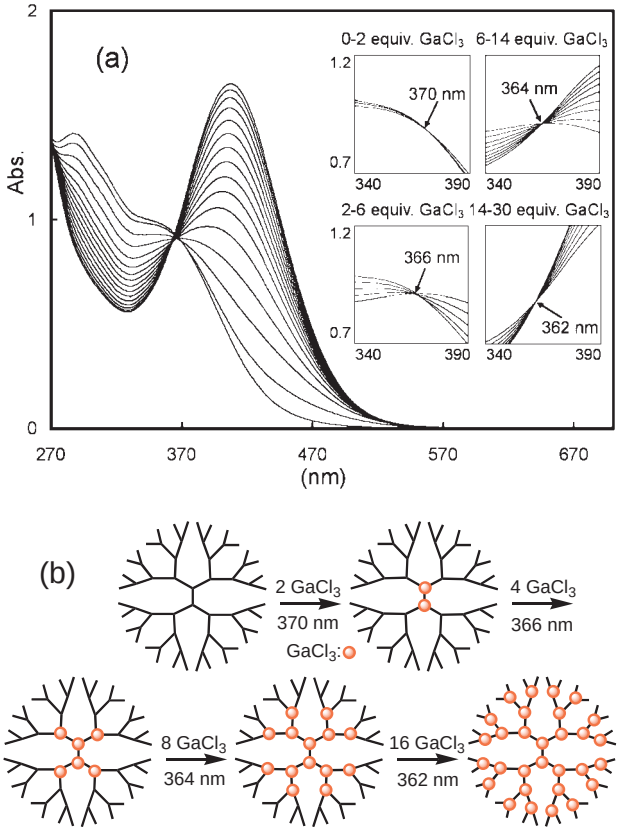

Fig. 2. (a) UV–vis titration of DPA G4 (5.0×10^{-6} M, acetonitrile/chloroform = 1:1) with $GaCl_3$ (5.0×10^{-3} M, acetonitrile) showing the detailed spectra around the isosbestic points (inset). (b) Schematic representation of stepwise complexation of DPA G4 with $GaCl_3$.

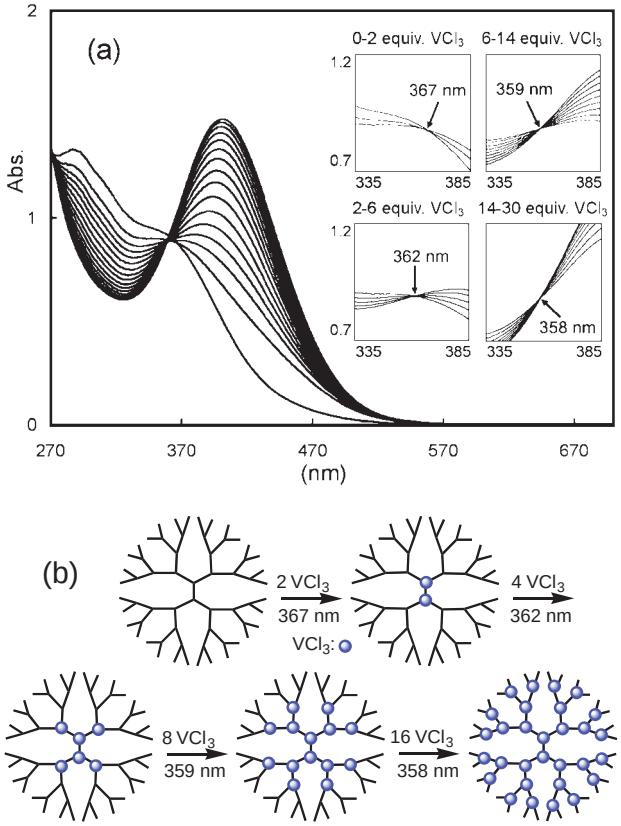

Fig. 3. (a) UV–vis titration of DPA G4 (5.0×10^{-6} M, acetonitrile/chloroform = 1:1) with VCl_3 (5.0×10^{-3} M, acetonitrile) showing the detailed spectra around the isosbestic points (inset). (b) Schematic representation of stepwise complexation of DPA G4 with VCl_3.

UV–vis spectroscopy. In the case of $GaCl_3$ (Fig. 2), the color of the DPA solution (5.0×10^{-6} M, acetonitrile/chloroform = 1:1) changed with the addition of $GaCl_3$ (5.0×10^{-3} M, acetonitrile) based on the complexation of imine and metal. With the addition of 0–2 equiv of $GaCl_3$, the isosbestic point was identified at 370 nm. However, the isosbestic points shifted to lower values with further addition of $GaCl_3$ to 366 nm at 2–6 equiv, 364 nm at 6–14 equiv, and 362 nm at 14–30 equiv. The observation of four discrete isosbestic points suggests that four different types of complexation occurred in this process. This behavior is similar to that for $SnCl_2$ and $FeCl_3$.[8–10] The equivalent amounts for each step were 2, 4, 8, and 16, corresponding to the number of each layer of imine sites. This demonstrates that $GaCl_3$ can complex with DPA in the same stepwise fashion as $SnCl_2$ and $FeCl_3$. This stepwise complexation was also observed for DPA G2 and G3 (Fig. S1), where two and three isosbestic points were observed during the titration, respectively.

Further, in the case of VCl_3 (Fig. 3), the isosbestic point shifted by 4 points (367 nm at 0–2 equiv, 362 nm at 2–6 equiv, 359 nm at 6–14 equiv, 358 nm at 14–30 equiv). The agreement of the equivalent amounts for each step and the number of each layer of imine sites shows a stepwise radial complexation from the inner to outer layers. These were also observed for DPA G2 (Fig. S2). Moreover, the Job-plot[13–15] was examined for $GaCl_3$ with imine on DPA G0 (Fig. S3). The maximum value in the Job plot appeared at a mole fraction of 0.5 indicating the formation of a 1:1 complex. This result supports quantitative complexation under titration conditions.

The complexation abilities of four metal salts, that is, $FeCl_3$, $GaCl_3$, VCl_3, and $SnCl_2$, were evaluated in a 1:1 acetonitrile/tetrahydrofuran[16] solution of DPA G1 using curve-fitting of a theoretical simulation for the titration[17] (Fig. 4). The results indicated that the order of complexation ability was as follows: $FeCl_3 > GaCl_3 > VCl_3 > SnCl_2$. $FeCl_3$ showed the largest equilibrium constant for the complexation (K) between metal salt and imine, which was determined to be $10^5\,M^{-1}$. $SnCl_2$ showed the smallest one ($K = 10^3\,M^{-1}$). The difference in K was found to be an important factor in heterometal assembly.

Heterometal Assembling on DPA. The above results demonstrate the stepwise radial complexation of DPA with $GaCl_3$ and VCl_3. The complexation ability decreased in the order $FeCl_3 > GaCl_3 > VCl_3 > SnCl_2$. As an extension of the previous work on the assembly of a single metal salt on DPA, the assembly of two kinds of metals was attempted.

DPA undergoes stepwise complexation with metals by complexing with imines sequentially from the inner layer to the outer layer following the gradients of electric charge density.[8–10] The coordination of different metal salts will occur in a sequence determined by the coordination constants between the metal salts and the imine layers. First, layer-selective heterometal assembly[18–20] on DPAs was examined in this study

with a combination of $FeCl_3$ and $SnCl_2$, which have different coordination constants ($K_{FeCl3} = 10^5\,M^{-1}$, $K_{SnCl2} = 10^3\,M^{-1}$).

We first performed the UV–vis titration by the addition of $FeCl_3$ followed by $SnCl_2$ using DPA G4 (5.0×10^{-6} M, acetonitrile/chloroform = 1:1, Fig. 5).[10] After adding 6 equiv of $FeCl_3$, the isosbestic points were observed at 371 nm for 0–2 equiv of $FeCl_3$ and 369 nm for 2–6 equiv of $FeCl_3$, which correspond to the complexation of 1–2 layers. After adding $SnCl_2$, the isosbestic points shifted to 364 nm for 0–8 equiv of $SnCl_2$ and to 363 nm for 8–24 equiv of $SnCl_2$, which correspond to the complexation of 3–4 layers (Figs. 5a and 5b-(2)). Similarly, adding 2 equiv of $FeCl_3$ followed by 28 equiv of $SnCl_2$, the isosbestic points shifted an equivalent amount for each step, corresponding to the number of 2–4 layers of imine sites for $SnCl_2$ (Fig. 5b-(1), Fig. S4). Adding $FeCl_3$ to the third layer followed by $SnCl_2$, the isosbestic point shifted one point during addition of $SnCl_2$, which means $SnCl_2$ accumulated on the fourth layer (Fig. 5b-(3), Fig. S4). These results indicate that $SnCl_2$ accumulated on the outer layer and did not exchange with $FeCl_3$ at complex sites (Fig. 5 and Fig. S4). Another combination of metals was examined and similar results were obtained (Fig. S5 and Table 1).

However, in case of the addition of $SnCl_2$ followed by $FeCl_3$, the shift in the isosbestic points was different from the case of $FeCl_3$ followed by $SnCl_2$ (Fig. 6). If the metal salts were assembled according to the order of addition of the metal salts, $FeCl_3$ would be present in the third layer, and the isosbestic point during the addition of $FeCl_3$ would not change. But, adding 6 equiv of $SnCl_2$ to the second layer, followed by 6 equiv of $FeCl_3$, the isosbestic points during addition of $FeCl_3$ were observed at 361 nm for 0–2 equiv of $FeCl_3$ and 359 nm for 2–6 equiv of $FeCl_3$. The clear change in the isosbestic point therefore indicates that the heterometal complexation is not governed by the order of addition of the metals. Equivalent values for each isosbestic point during $FeCl_3$ were

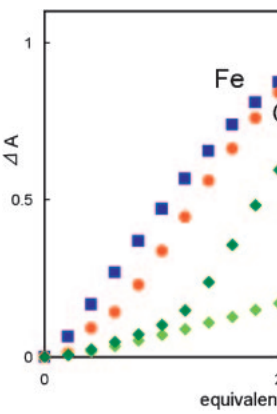

Fig. 4. Titration curves of DPA G1 (5.0×10^{-5} M, tetrahydrofuran/acetonitrile = 1:1) complexed with $FeCl_3$, $GaCl_3$, VCl_3, and $SnCl_2$. Optical difference at the band attributed to the complexation during the titration was normalized as ΔA.[29] The complexation abilities of four metal salts were derived by curve-fitting a theoretical simulation to the titration.

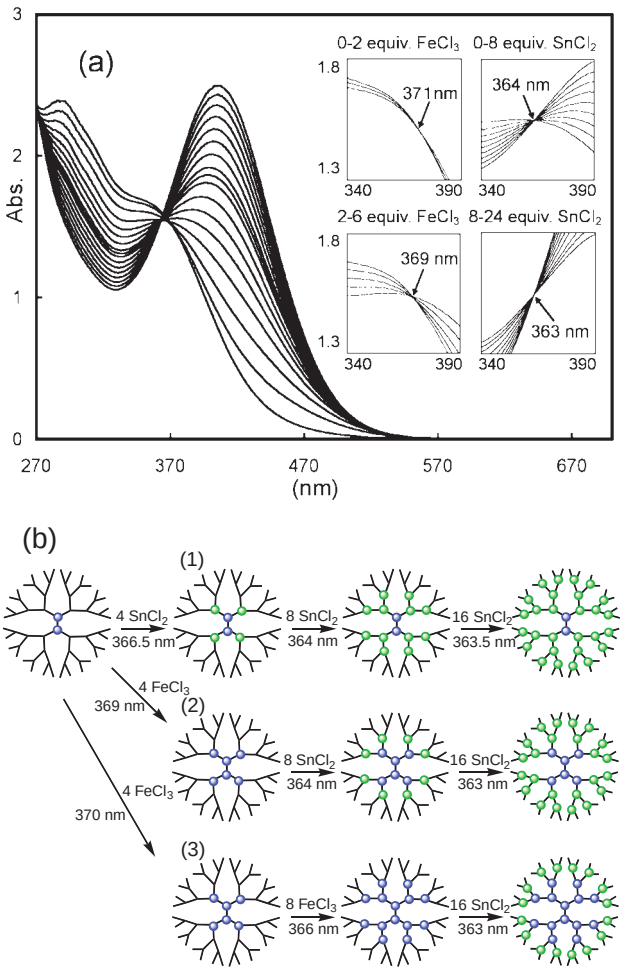

Fig. 5. (a) Heterometal assembly of DPA G4 (5.0×10^{-6} M, acetonitrile/chloroform = 1:1) by the addition of 6 equiv of $FeCl_3$ followed by 24 equiv of $SnCl_2$. Detailed spectra of the isosbestic points are inset. These spectra correspond to the schematic representation of the pattern (1). The other spectra which correspond to the schematic representation of the pattern (2) and (3) are shown in Fig. S4. (b) Schematic representation of heterometal assembly on DPA G4 by the addition of $FeCl_3$ followed by $SnCl_2$.

Table 1. Isosbestic Points during the Titration of DPA G4 with Two Metals ($FeCl_3$, $GaCl_3$, and $SnCl_2$)

	2Fe → 28Ga /nm	6Fe → 24Ga /nm	14Fe → 16Ga /nm	2Fe → 28Sn /nm	6Fe → 24Sn /nm	14Fe → 16Sn /nm	2Ga → 28Sn /nm	6Ga → 24Sn /nm	14Ga → 16Sn /nm
1st (2 equiv)	370.5(Fe)	370.5(Fe)	371(Fe)	371(Fe)	371(Fe)	370.5(Fe)	370(Ga)	370(Ga)	370(Ga)
2nd (4 equiv)	368(Ga)	369(Fe)	369(Fe)	366.5(Sn)	369(Fe)	369(Fe)	366(Sn)	366(Ga)	366(Ga)
3rd (8 equiv)	365.5(Ga)	368(Ga)	366(Fe)	364(Sn)	364(Sn)	366(Fe)	365(Sn)	364(Sn)	364(Ga)
4th (16 equiv)	363.5(Ga)	365.5(Ga)	370(Ga)	363.5(Sn)	363(Sn)	363(Sn)	363(Sn)	363(Sn)	362(Sn)

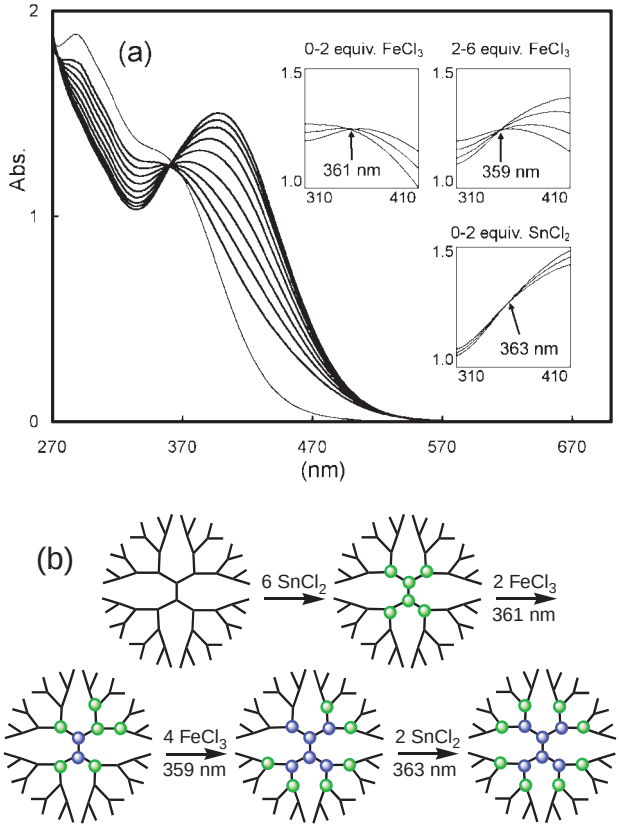

Fig. 6. (a) Heterometal assembly of DPA G4 (5.0×10^{-6} M, acetonitrile/chloroform = 1:1) by the addition of 6 equiv of $SnCl_2$ followed by 6 equiv of $FeCl_3$ and 2 equiv of $SnCl_2$. Detailed spectra of the isosbestic points are inset. (b) Schematic representation of heterometal assembly on DPA G4 by the addition of $SnCl_2$ followed by $FeCl_3$.

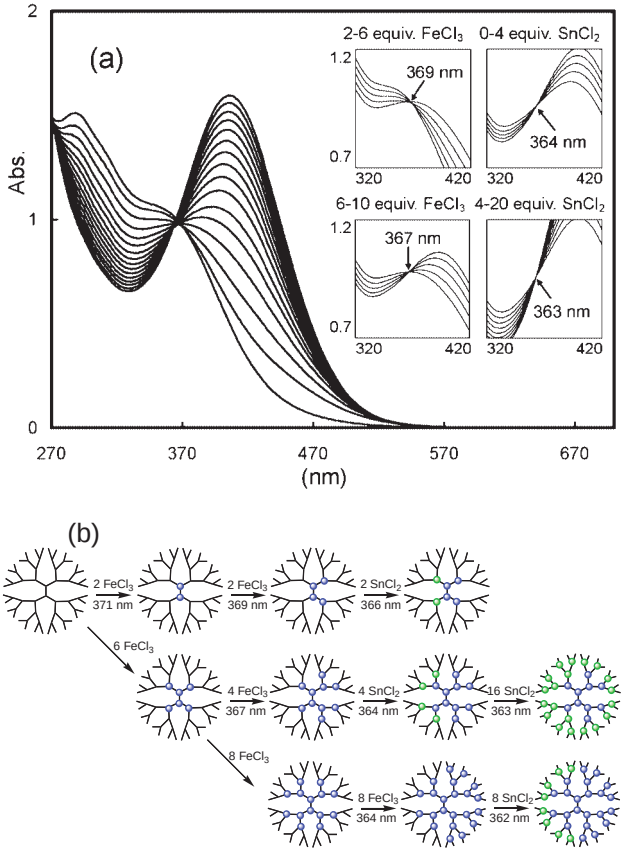

Fig. 7. (a) Heterometal assembly of DPA G4 (5.0×10^{-6} M, acetonitrile/chloroform = 1:1) by the addition of 10 equiv of $FeCl_3$ followed by 4 equiv of $SnCl_2$. Detailed spectra of the isosbestic points are inset. The other patterns are shown in Fig. S7. (b) Schematic representation of heterometal assembly on the same layer of DPA G4 with the addition of $FeCl_3$ followed by $SnCl_2$.

2 and 4, which correspond to the number of first and second layers of imine sites (Fig. 6); therefore $SnCl_2$ on the first and second layer moved to the third layer with the addition of $FeCl_3$. We also examined the pattern of $SnCl_2$ followed by $GaCl_3$, and a similar result was obtained (Fig. S6).

Moreover, we examined the accumulation of two kinds of metals on the same layer. Upon adding $FeCl_3$ followed by $SnCl_2$ to the same layer, two isosbestic points were observed, one derived from $FeCl_3$ and the other from $SnCl_2$ (Fig. 7 and Fig. S7). A similar pattern occurred even if the combination of metal salts was changed (Fig. S8). Therefore, different isosbestic points appeared when different metal salts were mixed in the same DPA layer.

On the other hand, adding 8 equiv of $SnCl_2$ followed by 6 equiv of $FeCl_3$ to the same layer, two isosbestic points were observed at 360 nm for 0–2 equiv of $FeCl_3$ and 362 nm for 2–6 equiv of $FeCl_3$. This indicates that $FeCl_3$ drives out $SnCl_2$ on both the first layer and the second layer (Fig. 8). In addition, the location and type of metals was confirmed in the UV–vis spectra, because two isosbestic points were observed when two metals filled in the layer.

We used UV–vis spectroscopy to confirm that the complex reaches the same final state regardless of the order of addition. We investigated the final states of the complexes incorporating 6 equiv of $FeCl_3$ and 8 equiv of $SnCl_2$ in DPA G4 (5.0×10^{-6} M, acetonitrile/chloroform = 1:1) with these three patterns: [$6FeCl_3 \rightarrow 8SnCl_2$], [$6SnCl_2 \rightarrow 6FeCl_3 \rightarrow 2SnCl_2$], and [$8SnCl_2 \rightarrow 6FeCl_3$]. The resulting spectra were in agreement ($\lambda_{max} = 397$ nm, $\varepsilon = 2.5 \times 10^5$ dm^3 mol^{-1} cm^{-1}) (Fig. 9). In addition, the spectra agreed for the combination of 6 equiv of $GaCl_3$ and 8 equiv of $SnCl_2$, (Fig. S9). For heterometal assembly in DPA using $FeCl_3$ and $SnCl_2$, regardless of the order of addition of the metals, $FeCl_3$ complexed in the interior layer of DPA G4, whereas $SnCl_2$ complexed in the exterior layer. This result indicates that the complex reaches a thermodynamically stable condition regardless of the order of addition. This result can be attributed to the difference in K between $FeCl_3$ and $SnCl_2$, where the metal with the larger K complexes with the inner layer imines, and the metal with the smaller K coordinates with the outer layer imines.

Based on this principle, heterometal assembly with $FeCl_3$, $GaCl_3$, VCl_3, and $SnCl_2$ was carried out. As the titration was carried out in the order of complexation ability, four shifts in isosbestic points (371 nm → 368 nm → 356 nm → 364 nm) were observed (Fig. 10). This indicates that the complexation is in a stepwise radial fashion, because the added metal equivalents, 2, 4, 8, and 16 corresponded to the number of complexation sites in each layer of DPA (Fig. 10). Various patterns of

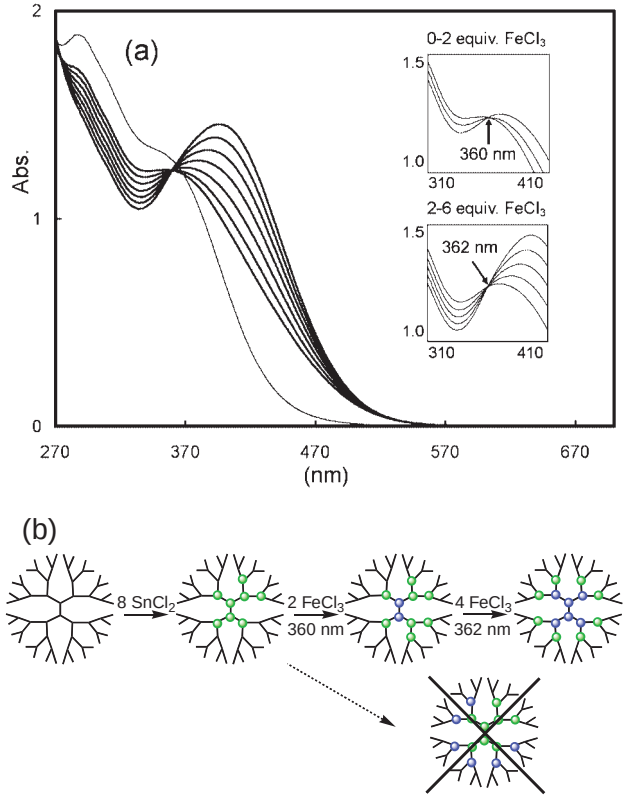

Fig. 8. (a) Heterometal assembly of DPA G4 (5.0×10^{-6} M, acetonitrile/chloroform = 1:1) by the addition of 8 equiv of $SnCl_2$ followed by 6 equiv of $FeCl_3$. Detailed spectra of the isosbestic points are inset. (b) Schematic representation of heterometal assembly of DPA G4 by the addition of $SnCl_2$ followed by $FeCl_3$.

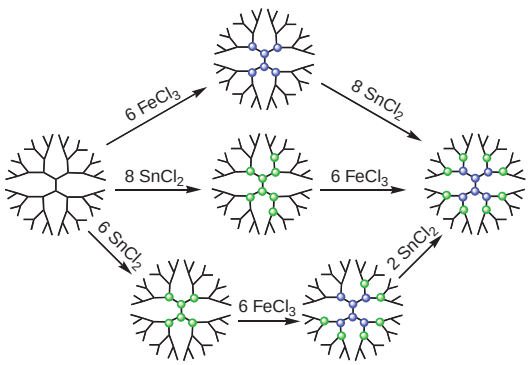

Fig. 9. Schematics of the addition of the metal salts in the following order: [$6FeCl_3 \rightarrow 8SnCl_2$; $\lambda_{max} = 397$ nm, $\varepsilon = 2.5 \times 10^5$ dm^3 mol^{-1} cm^{-1} (based on the concentration of DPA G4 (5.0×10^{-6} M, acetonitrile/chloroform = 1:1)], [$8SnCl_2 \rightarrow 6FeCl_3$; $\lambda_{max} = 397$ nm, $\varepsilon = 2.5 \times 10^5$ dm^3 mol^{-1} cm^{-1}] and [$6SnCl_2 \rightarrow 6FeCl_3 \rightarrow 2SnCl_2$; $\lambda_{max} = 397$ nm, $\varepsilon = 2.5 \times 10^5$ dm^3 mol^{-1} cm^{-1}].

metals were examined (Table 2). We succeeded in developing a method of heterometal assembly incorporating different metal salts in each of four layers. From these results, heterometal assembling on DPA appears to be governed by the complexation ability of metal salts, with the stronger coordinating

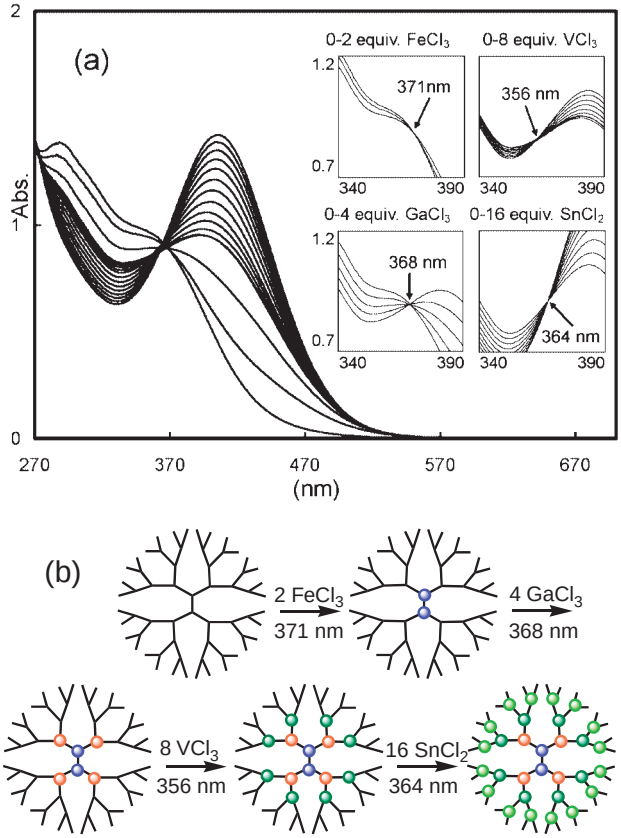

Fig. 10. (a) UV–vis titration of DPA G4 (5.0×10^{-6} M, acetonitrile/chloroform = 1:1) with $FeCl_3$, $GaCl_3$, VCl_3, and $SnCl_2$. (b) Schematic representation of heterometal assembly of DPA G4 by $FeCl_3$, $GaCl_3$, VCl_3, and $SnCl_2$.

Table 2. Isosbestic Points during the Titration of DPA G4 with Three Different Metals ($FeCl_3$, $GaCl_3$, and $SnCl_2$)

$1 \rightarrow 2 \rightarrow 3 \rightarrow 4$	Fe, Fe, Ga, Sn /nm	Fe, Ga, Ga, Sn /nm	Fe, Ga, Sn, Sn /nm
1st (2 equiv)	370(Fe)	370.5(Fe)	370(Fe)
2nd (4 equiv)	366.5(Fe)	366.0(Ga)	365.5(Ga)
3rd (8 equiv)	364.5(Ga)	364.5(Ga)	364.0(Sn)
4th (16 equiv)	363.5(Sn)	363.5(Sn)	362.5(Sn)

metal in the inner layer and the weaker coordinating metal in the outer layer.

TEM Observation of Dendrimer Metal Assemblies. Since TEM can observe only metal assemblies, it is a useful technique for studying our heterometal dendrimer assemblies. Since metals are assembled stepwise from the interior of a dendrimer, the assembly areas should be different depending on the number of metals assembled. Generally in TEM observation, organic substances are dyed with RuO_4 vapor to intensify the visual contrast. However, tin and some other metals assembled in an organic substance are observable without dyeing or by dyeing for a very short time. We began with the TEM observation of DPA G4 assembled with 14 equiv $FeCl_3$ ($(FeCl_3)_{14}$@DPA G4) and 14 equiv $FeCl_3$ and 16 equiv $SnCl_2$ ($(FeCl_3)_{14}(SnCl_2)_{16}$@DPA G4) (Fig. 11).[8,9] We measured the

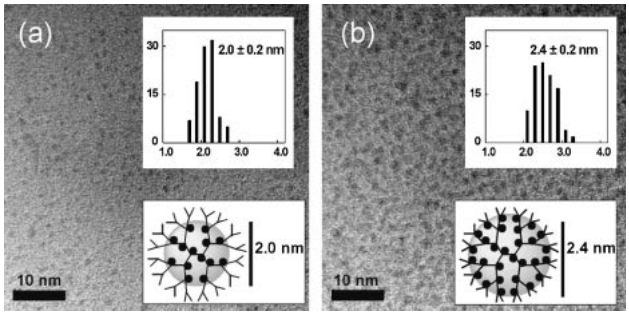

Fig. 11. TEM observation of dendrimer metal assemblies. (a) $(FeCl_3)_{14}$@DPA G4 was dyed for a short time, and the metal assembly was observed. (b) $(FeCl_3)_{14}$-$(SnCl_2)_{16}$@DPA G4 was dyed for a short time, and the metal assembly was observed.

sizes of the metal assemblies in $(FeCl_3)_{14}$@DPA G4 and estimated their average diameter to be 2.0 nm, and that in $(FeCl_3)_{14}(SnCl_2)_{16}$@DPA G4 to be 2.4 nm. As the number of metals increased, the assembly areas expanded. The size of the metal assembly in $(FeCl_3)_{14}$@DPA G4 matched that in $(SnCl_2)_{14}$@DPA G4, which we have reported earlier.[8,9] This size covers the metal assemblies up to the third layer inside the dendrimer and suggests that the 14 metals are assembled in the first through the third layers from the center of the dendrimer, and not randomly over the four layers. On the other hand, the size of the metal assembly in $(FeCl_3)_{14}(SnCl_2)_{16}$@DPA G4 was 0.4 nm larger than that in $(FeCl_3)_{14}$@DPA G4, which suggests that some tin filled the fourth layer.[21]

Next, we dyed $(FeCl_3)_{14}$@DPA G4 and $(FeCl_3)_{14}(SnCl_2)_{16}$@DPA G4 for about 15 min and observed the sizes of the whole dendrimer molecules (Fig. S10). We estimated the sizes to be 2.5 nm for the $(FeCl_3)_{14}$@DPA G4 molecule and 2.7 nm for $(FeCl_3)_{14}(SnCl_2)_{16}$@DPA G4. These values are larger than the metal areas and the sizes of assemblies in $(FeCl_3)_{14}$@DPA G4 and $(FeCl_3)_{14}(SnCl_2)_{16}$@DPA G4 are correct.[8,9]

As a result of the above, we have shown that the size of the metal-coordinated sections as well as the molecules created increases as a result of metal assembly in dendrimers, even when different kinds of metals are assembled. This fact suggests that the metals complex stepwise from the inside of the dendrimer.

^{57}Fe Mössbauer Spectra of DPA Complexes. In order to clarify the precise structure of the heterometal assembly, we measured Mössbauer spectra of ^{57}Fe (Fig. 12). To obtain $(^{57}FeCl_3)_2$@DPA G4, we formed a complex of $^{57}FeCl_3$ and DPA G4, brought it into a state of equilibrium, and then precipitated it into hexane. Figure 12 shows the Mössbauer spectra of the powdered solids that we obtained by treating $(^{57}FeCl_3)_2$@DPA G4, $(^{57}FeCl_3)_6$@DPA G4, and $(^{57}FeCl_3)_2$-$(SnCl_2)_4$@DPA G4 in a similar way. (In Fig. S11, the spectra were normalized with respect to intensity.) $(FeCl_3)_2$@DPA G4 shows a spectrum different from that of $FeCl_3$ alone (IS = 0.436, QS = 0 at RT).[22] This is due to the complex formation of $FeCl_3$ with imine. The $(FeCl_3)_2$@DPA G4 spectra shows no temperature dependence (Fig. S12). In addition, the IS and QS values indicate the high-spin state of Fe.[23]

A single doublet-fitting was used with the spectrum of $(FeCl_3)_2$@DPA G4 (IS = 0.30, QS = 0.80) and indicates the existence of a single component, Fe. On the other hand, for

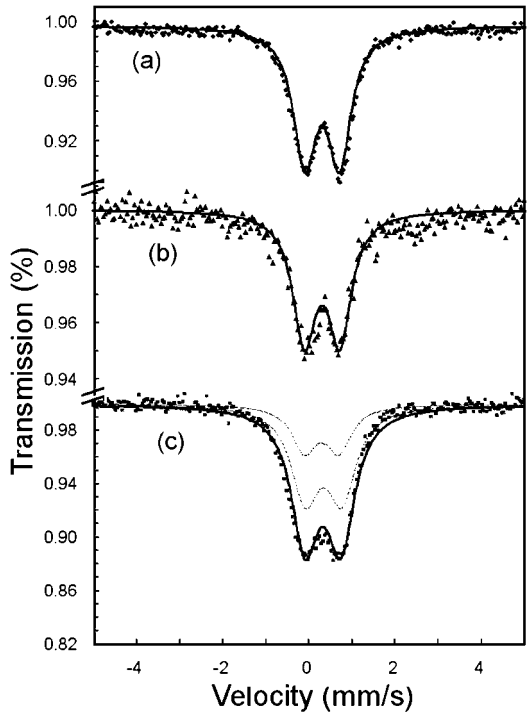

Fig. 12. ^{57}Fe Mössbauer spectra of: (a) $(FeCl_3)_2$@DPA G4 (IS = 0.30, QS = 0.80), (b) $(FeCl_3)_2(SnCl_2)_4$@DPA G4 (IS = 0.30, QS = 0.80), and (c) $(FeCl_3)_6$@DPA G4 (IS = 0.30, QS = 0.80, IS = 0.34, QS = 0.85). $(FeCl_3)_2$ @DPA G4 and $(FeCl_3)_2(SnCl_2)_4$@DPA G4 exhibit very similar spectra, which indicates that the Fe environments are similar. On the other hand, the peak for $(FeCl_3)_6$@DPA G4 is flat (see Fig. S15), indicating that it is a mix of two components.

$(FeCl_3)_6$@DPA G4, a two-doublet fitting was needed (IS = 0.30, QS = 0.80, IS = 0.34, QS = 0.85). These results suggest that Fe is attached only to the core of $(FeCl_3)_2$@DPA G4. Results for $(FeCl_3)_6$@DPA indicate the existence of a component coordinated in the first layer and another component in the second layer. This conclusion is also supported by the fact that two-component fitting was certainly possible in the analysis of the spectrum of $(FeCl_3)_6$@DPA G4 based on the parameters for $(FeCl_3)_2$@DPA G4, with a 1:2 ratio between the two components.

$(FeCl_3)_2(SnCl_2)_4$@DPA G4 exhibits a spectrum very similar to that of $(FeCl_3)_2$@DPA G4. $(FeCl_3)_2(SnCl_2)_4$@DPA G4 is also a single doublet, and we were able to fit it by using parameters from $(FeCl_3)_2$@DPA G4. This result shows that the environment for the Fe is the same as that in $(FeCl_3)_2$@DPA G4 and indicates that the Fe in $(FeCl_3)_2(SnCl_2)_4$@DPA G4 is not randomly placed, but attached to the core.

The results described above demonstrate that the $FeCl_3$ complex forms stepwise from the center, and that the hetero assembly consists of precisely located Fe and Sn atoms.

X-ray Photoelectron Spectra of Dendrimer Complexes. In XPS observation of a metal complex, the more intense the electron donation from the ligand, the lower the eV at which the metal ion's spectrum peak is observed.[24] When the position of the metal located in the DPA changes, the spectra also changes corresponding to the difference in the electric charge

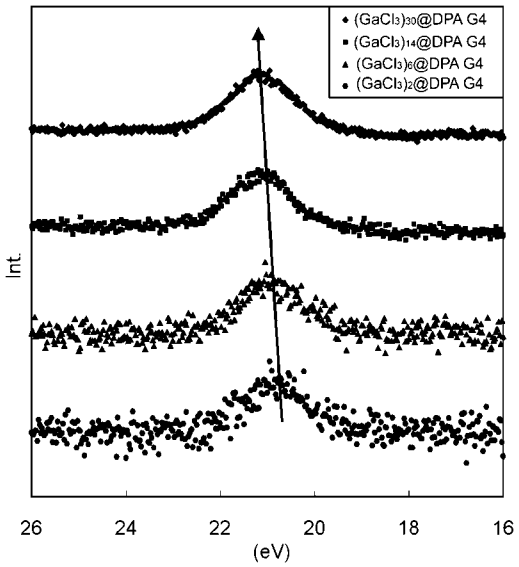

Fig. 13. $Ga_{3d3/2}$ XPS spectra of $(GaCl_3)_2$@DPA G4 (20.75 eV), $(GaCl_3)_6$@DPA G4 (20.90 eV), $(GaCl_3)_{14}$@DPA G4 (21.05 eV), and $(GaCl_3)_{30}$@DPA G4 (21.15 eV). As $GaCl_3$ increased, the spectral peaks shifted to a higher electronvolts.

density. Due to its detection sensitivity, $GaCl_3$[$Ga(3d_{3/2})$] was the metal of choice, and its assemblies were produced in DPA (Fig. 13). The UV–vis spectrum of $GaCl_3$ changes stepwise. Based on this change, we synthesized $(GaCl_3)_2$@DPA G4, $(GaCl_3)_6$@DPA G4, $(GaCl_3)_{14}$@DPA G4, and $(GaCl_3)_{30}$@DPA G4 and conducted XPS measurements on the assemblies.

The top peak in the spectrum of $Ga(3d_{3/2})$ shifted upwards from 20.75 to 20.90, 21.05, and 21.15 eV as the metal assembly increased from 2 to 6, 14, and 30, respectively. Simulations were performed on how the assembly takes place and how the spectrum changes (Fig. S13). If the metals assemble randomly in the different layers of imine sites, the spectrum shows no change even when the number of metals assembled increases. Only when different layers of imine sites have different electron-donating properties and the metals assemble stepwise from the inside do the peaks shift to higher energy. Since this agrees with our experimental results, it is evident that the metal assembly had some regularity. The spectral peak shifted towards higher energy as the assembly increased, which indicates a decrease in average electric charge density of the metal captured into the dendrimer. In more specific terms, this fact indicates that as metals add, they firstly assembled in the inner layer of imines, where the charge density is high, followed by assembly into the outer layer where the charge density is lower. We observed similar shifts in peaks in the XPS spectra of $(SnCl_2)_n$@DPA G4 [Fig. S14 for $(SnCl_2)_2$@DPA G4 (487.10 eV), $(SnCl_2)_6$@DPA G4 (487.25 eV), $(SnCl_2)_{14}$@DPA G4 (487.30 eV), and $(SnCl_2)_{30}$@DPA G4 (487.35 eV)]. These results also prove that the metals form a complex from the inner layer.

NMR Spectroscopy. BF_3 assembled stepwise in DPA G4 in four layers, beginning with the innermost one. Figure S15 shows the UV–vis titrations. We estimated K to be equal to or larger than that of $FeCl_3$ ($K > 10^8\,M^{-1}$, Figs. S16–S19). We measured the ^{19}F NMR spectrum of BF_3 introduced into

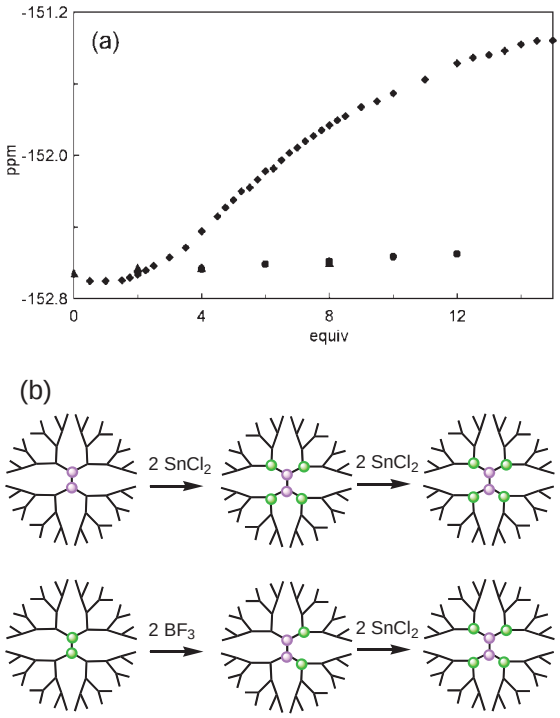

Fig. 14. (a) Chart showing the relationship between the chemical shift of the fluorine peak in the ^{19}F NMR spectrum and the quantity of BF_3 added (indicated as ◆). Also shown is the relationship in the case of adding $SnCl_2$ to $(BF_3)_2$@DPA G4, with the vertical axis denoting the chemical shift and the horizontal axis the quantity of $SnCl_2$ added (indicated as ●). Similarly, a relationship is also shown for the case of adding $SnCl_2$ after adding two equivalent amounts of BF_3 to $(SnCl_2)_2$@DPA G4 (indicated as ▲). (b) Schematic representation of adding $SnCl_2$ to $(BF_3)_2$@DPA G4 and 2 equivalent amounts of BF_3 to $(SnCl_2)_2$@DPA G4.

the DPA.[25] At NMR concentrations, a complex formed more than 99% of the time.

Spectra were collected at room temperature. We added the BF_3 solution dropwise (0.25 equiv for each drop) into the DPA G4 solution (acetonitrile/chloroform = 1:1, 1.0×10^{-4} M) and measured the NMR spectra with trifluoroacetic acid as an external standard (−76.5 ppm).

With BF_3 alone, the peak appears at −150.5 ppm. With 0.25 equivalents of BF_3 added to the DPA G4 solution, the peak appeared at −152.7 ppm, because of its coordination on the imine. This coordination to the imine suggests that the electric charge density of F increases. With more BF_3 added, the peak shifted to a higher chemical shift (Fig. 14, −152.7 to −151.5 ppm). During the titration from 0 to 14 equivalent amounts, up to the third layer, we observed only one peak. Though we saw no peak reflecting each of the layers, we think that this is because the coordination kinetics and the time scale of the NMR measurement are comparable, and averaged peaks were observed as expected. What is important here is that since BF_3 was almost completely incorporated into the complex, no shift in the F peak would have been seen if the chemical environment within the dendrimer had been consistent throughout or if BF_3 had been randomly placed (Fig. S20). The shift in the

F peak take place because the F atoms exists in different environments and are regularly assembled. The peak shifted upfield with addition of BF_3, suggesting that the electron density of F increases (more shielding). We propose that, since the electron density of the imine is lower in the outer layers, the downfield F peak shift (less shielding) indicates more BF_3 is coordinated in the outer layers. This result suggests the existence of an electron gradient of nitrogen from the inner to the outer layers.

BF_3 has the largest complexation constant of all the metals that gradually form a complex with DPA. Therefore, BF_3 remained in the inner layers even after mixing with another metal. Despite the addition of a heterometal, the chemical shift remains the same. We added some Sn after adding 2 equivalents of BF_3 and then observed the chemical shift. We found the chemical shift remained the same, regardless of the quantity of Sn added (Fig. 14). Similarly, we found that the chemical shift was the same for $(SnCl_2)_2$@DPA G4 with 2 equivalent amounts of BF_3 added and after adding $SnCl_2$ to the mixture (Fig. 14). These results also suggest that in the assemblies of heterometals, BF_3 assembles in the inner layers and $SnCl_2$ in the outer layers. In other words, the assembly structure is metals with a higher K in the inner layers and metals with a lower K in the outer layers.

Conclusion

We demonstrated the stepwise complexation of $GaCl_3$ and VCl_3 on DPA by the shifts of isosbestic points of UV–vis spectra. Further, we developed a method of precise heterometal assembly, which makes use of these different complexation abilities ($FeCl_3 > GaCl_3 > VCl_3 > SnCl_2$). The stepwise complexation and heterometal assembling were also supported by TEM, ^{57}Fe Mössbauer spectroscopy, XPS measurements, and NMR spectroscopy. These methods may be used to generate new materials and could be applied to many fields, such as catalysts and electronics.

Experimental

Materials. DPAs were prepared according to the reported method.[26,27] Dehydrated chloroform and tin(II) chloride were purchased from Wako Pure Chemical industries (Japan), dehydrated acetonitrile and $BF_3 \cdot OEt_2$ were purchased from Kanto Kagaku (Japan), iron(III) chloride was purchased from Merck, and gallium(III) chloride and vanadium(III) chloride were purchased from Sigma-Aldrich. ^{57}Fe was purchased from TANGO OVERSEAS (Japan) and $^{57}FeCl_3$ was prepared according to the literature method.[28]

General Method. UV–vis spectra were measured using Shimadzu UV-3150, UV-3100PC, and UV-2400PC spectrophotometers. The ^{57}Fe Mössbauer spectra were measured using a Topologic systems model 222 constant-acceleration spectrometer with a ^{57}Co/Rh source in the transmission mode. The measurements at low temperature were performed with a closed-cycle helium refrigerator (Daikin). The XPS measurements were performed using a JEOL JPS-9000MC spectrometer with a Mg Kα radiation. The TEM images were obtained using a TECNAI F20 field-emission electron microscope operated at 200 kV. The NMR spectra were measured using a JEOL JNM-A400 spectrometer.

UV–Vis Titration. Solutions of DPA G4 (acetonitrile/chloroform = 1:1, 5.0×10^{-6} M), $FeCl_3$ (acetonitrile, 5.0×10^{-3} M), $GaCl_3$ (acetonitrile, 5.0×10^{-3} M), $SnCl_2$ (acetonitrile, 5.0×10^{-3} M), and VCl_3 (acetonitrile, 5.0×10^{-3} M) were prepared in volumetric flasks under nitrogen. To a quartz cell was added 3.0 mL of the DPA G4 solution, followed by the addition of 3 μL of metal salt solution (i.e., 1 equivalent for DPA G4). The UV–vis spectra were measured until agreement was obtained with the one immediately before. Measurements were repeated after each addition of 3 μL of metal salt solution to achieve UV–vis titration. In the case of $FeCl_3$, the absorbance of $FeCl_3$ was subtracted.[10]

Job Plot of DPA G0 Imine and $GaCl_3$. A Job plot of the reaction between $GaCl_3$ and DPA G0 was done. $F(x) = \text{Abs.}/(C_{G0} + C_{GaCl3}) - (\varepsilon_{G0} - \varepsilon_{GaCl3})x - \varepsilon_{GaCl3}$, $x = C_{G0}/(C_{G0} + C_{GaCl3})$; mole fraction of DPA G0. Solutions of DPA G0 (acetonitrile/chloroform = 1:1, 2.5×10^{-4} M^{-1}) and $GaCl_3$ (acetonitrile/chloroform = 1:1, 2.5×10^{-4} M^{-1}) were prepared in volumetric flasks, the latter under nitrogen. To a quartz cell was added 2.0 mL of the DPA G0 solution followed by the sequential addition of 0.2 mL aliquots of the $GaCl_3$ solution up to a total of 2.2 mL to obtained solutions mixed in various proportions. The UV–vis spectra were recorded between each step. The same operation was also performed by the addition of DPA G0 solution to the $GaCl_3$ solution. The plot shows a maximum at 0.5 mole fraction of DPA G0, which means that the imine forms a 1:1 complex with $GaCl_3$. The value of K, which was found by curve-fitting a theoretical simulation to the experimental data was more than 10^8 M^{-1} (in acetonitrile/chloroform).

Titration of DPA G1 with Metals in Acetonitrile/Tetrahydrofuran = 1:1 Solvent. Solutions of DPA G1 (acetonitrile/tetrahydrofuran = 1:1, 5.0×10^{-5} M), $FeCl_3$ (acetonitrile, 1.0×10^{-2} M), $GaCl_3$ (acetonitrile, 1.0×10^{-2} M), $SnCl_2$ (acetonitrile, 1.0×10^{-2} M), and VCl_3 (acetonitrile, 1.0×10^{-2} M) were prepared in volumetric flasks under nitrogen. To a quartz cell was added 3.0 mL of the DPA G4 solution, followed by the addition of 3 μL of metal salt solution (i.e., 0.2 equivalent for DPA G1). The measurement of the spectra and the addition of the metal salt solution continued until the spectral change stopped.

XPS Measurements of DPA Complexes. To a 1 mL solution of DPA G4 (acetonitrile/chloroform = 1:1, 5×10^{-4} M), 2, 6, 14, or 30 equiv $GaCl_3$ solution (acetonitrile, 2.0×10^{-2} M) was added. This $GaCl_3$@DPA G4 solution (10 μL) was then applied to the Au plates (7×7 mm^2) and dried in vacuo. The samples were characterized by the Ga(3d) peak. The Au($3f_{7/2}$) peak was used as an internal standard (83.8 eV).

TEM Observation of DPA Complexes. TEM samples were prepared by applying 1.5 μL of the solution of $(FeCl_3)_{14}$@DPA G4 or $(FeCl_3)_{14}(SnCl_2)_{16}$@DPA G4 (chloroform, 1×10^{-5} M) to two carbon-coated TEM grids and dried in vacuo. One plate was treated by RuO_4 vapor for 1 min and the other was treated for 15 min. The TEM images were obtained at 200 kV and the size distribution of particles was determined by counting about 100 particles.

^{57}Fe Mössbauer Spetra. All samples were prepared using $^{57}FeCl_3$. The samples of $(FeCl_3)_2$@DPA G4, $(FeCl_3)_2(SnCl_2)_4$@DPA G4, and $(FeCl_3)_6$@DPA G4 were prepared by reprecipitation from hexane. A typical preparation of $(FeCl_3)_2$@DPA G4 was as follows. 7.0 mg of $^{57}FeCl_3$ (7.0 mg, 43.5 μmol) was dissolved in (1.0 mL) and 0.128 mL of this solution was added to the solution of DPA G4 (15 mg, 2.75 μmol, chloroform:acetonitrile = 1:1, 3 mL). This Fe–DPA complex solution was poured into 300 mL of hexane with sonication, and the precipitate was collected by membrane filtration. The samples were dried in vacuo and wrap-

ped in aluminum foil to perform the measurements. RT data for $(FeCl_3)_2$@DPA G4 were also collected. The spectra were analyzed by fitting a Lorentzian line shape using MOSSWINN version 3 software.

^{19}F NMR Spectra. Spectra were collected at room temperature. We adjusted the BF_3 solution by diluting $BF_3 \cdot OEt_2$ with acetonitrile. We added this solution dropwise (0.25 equiv for each drop) into a DPA solution (acetonitrile/chloroform = 1:1, 1.0×10^{-4} M) and measured the NMR spectra with trifluoroacetic acid as an external standard (−76.5 ppm). Similarly, we added $SnCl_2$ solution dropwise into a $(BF_3)_2$@DPA solution and measured the NMR specra. The case of adding $SnCl_2$ after adding two equivalent amounts of BF_3 to $(SnCl_2)_2$@DPA G4 was examined in the same way.

This work was partially supported by the CREST project from JST and Grants-in-Aid for Scientific Research (Nos. 19205020 and 178146) from the Ministry of Education, Culture, Sports, Science and Technology.

Supporting Information

UV–vis titration, Job-plot, TEM images, ^{57}Fe Mössbauer spectra, XPS spectra, and ^{19}F NMR chart. This material is available free of charge on the Web at: http://www.csj.jp/journals/bcsj/.

References

1 a) R. E. Blankenship, *Molecular Mechanisms of Photosynthesis*, Blackwell Science, Oxford, U.K., **2002**. b) A. E. Shilov, *Metal Complexes in Biomimetic Chemical Reactions*, Springer-Verlag, Berlin, Germany, **1997**. c) *Enzyme Catalysis in Organic Synthesis*, ed. by K. Drauz, H. Waldmann, VCH, Weinheim, Germany, **1995**.

2 a) *Macromolecular Metal Complexes*, ed. by F. Ciardelli, E. Tsuchida, D. Worle, Springer-Verlag, Berlin, Germany, **1995**. b) *Macromolecular Complexes*, ed. by E. Tsuchida, VCH, New York, **1991**. c) *Metal Containing Polymeric Materials*, ed. by C. U. Pittman, B. M. Cullberston, J. E. Sheet, ACS Symposium Series, Plenum, New York, **1996**.

3 a) D. Astruc, F. Chardac, *Chem. Rev.* **2001**, *101*, 2991. b) R. M. Crooks, M. Zhao, L. Sun, V. Chechik, L. K. Yeung, *Acc. Chem. Res.* **2001**, *34*, 181. c) R. van Heerbeek, P. C. J. Kamer, P. W. N. M. van Leeuwen, J. N. H. Reek, *Chem. Rev.* **2002**, *102*, 3717. d) M. Ooe, M. Murata, T. Mizugaki, K. Ebitani, K. Kaneda, *J. Am. Chem. Soc.* **2004**, *126*, 1604.

4 Reviews of dendrimer, see for example: a) F. Zeng, S. C. Zimmerman, *Chem. Rev.* **1997**, *97*, 1681. b) A. W. Bosman, H. M. Janssen, E. W. Meijer, *Chem. Rev.* **1999**, *99*, 1665. c) M. Fischer, F. Vögtle, *Angew. Chem., Int. Ed.* **1999**, *38*, 884. d) A. J. Berresheim, M. Müller, K. Müllen, *Chem. Rev.* **1999**, *99*, 1747. e) F. Vögtle, S. Gestermann, R. Hesse, H. Schwierz, B. Windisch, *Prog. Polym. Sci.* **2000**, *25*, 987. f) M. D. Watson, A. Fechtenkötter, K. Müllen, *Chem. Rev.* **2001**, *101*, 1267. g) S. M. Grayson, J. M. J. Fréchet, *Chem. Rev.* **2001**, *101*, 3819. h) G. R. Newkome, C. N. Moorefield, F. Vögtle, *Dendrimers and Dendrons: Concepts, Syntheses, Applications*, VCH, Weinheim, Germany, **2001**. i) J. M. J. Fréchet, D. A. Tomalia, *Dendrimers and Other Dendritic Polymers*, Wiley, Chichester, U.K., **2002**.

5 Catalysts using dendrimers, see for example: a) R. van Heerbeek, P. C. J. Kamer, P. W. N. M. van Leeuwen, J. N. H. Reek, *Chem. Rev.* **2002**, *102*, 3717. b) D. Astruc, F. Lu, J. R. Aranzaes, *Angew. Chem., Int. Ed.* **2005**, *44*, 7852. c) M. Kimura, T. Shiba, M. Yamazaki, K. Hanabusa, H. Shirai, N. Kobayashi, *J. Am. Chem. Soc.* **2001**, *123*, 5636. d) P. Weyermann, J.-P. Gisselbrecht, C. Boudon, F. Diederich, M. Gross, *Angew. Chem., Int. Ed.* **1999**, *38*, 3215. e) H. Zeng, G. R. Newkome, C. L. Hill, *Angew. Chem., Int. Ed.* **2000**, *39*, 1771. f) G. E. Oosterom, J. N. H. Reek, P. C. J. Kamer, P. W. N. M. van Leeuwen, *Angew. Chem., Int. Ed.* **2001**, *40*, 1828. g) M. Uyemura, T. Aida, *J. Am. Chem. Soc.* **2002**, *124*, 11392. h) J.-L. Zhang, H.-B. Zhou, J.-S. Huang, C.-M. Che, *Chem. Eur. J.* **2002**, *8*, 1554. i) L. Plault, A. Hauseler, S. Nlate, D. Astruc, J. Ruiz, S. Gatard, R. Neumann, *Angew. Chem., Int. Ed.* **2004**, *43*, 2924. j) K. Heuzé, D. Méry, D. Gauss, J.-C. Blais, D. Astruc, *Chem. Eur. J.* **2004**, *10*, 3936. k) S. A. Chavan, W. Maes, L. E. M. Gevers, J. Wahlen, I. F. J. Vankelecom, P. A. Jacobs, W. Dehaen, D. E. de Vos, *Chem. Eur. J.* **2005**, *11*, 6754.

6 Cluster synthesis using dendrimers, see for example: a) R. W. J. Scott, O. M. Wilson, R. M. Crooks, *J. Phys. Chem. B* **2005**, *109*, 692. b) Y. Niu, L. K. Yeung, R. M. Crooks, *J. Am. Chem. Soc.* **2001**, *123*, 6840. c) R. W. J. Scott, A. K. Datye, R. M. Crooks, *J. Am. Chem. Soc.* **2003**, *125*, 3708. d) R. W. J. Scott, O. M. Wilson, S.-K. Oh, E. A. Kenik, R. M. Crooks, *J. Am. Chem. Soc.* **2004**, *126*, 15583. e) J. C. Garcia-Martinez, R. M. Crooks, *J. Am. Chem. Soc.* **2004**, *126*, 16170. f) Y.-G. Kim, S.-K. Oh, R. M. Crooks, *Chem. Mater.* **2004**, *16*, 167. g) C. Wang, G. Zhu, J. Li, X. Cai, Y. Wei, D. Zhang, S. Qiu, *Chem. Eur. J.* **2005**, *11*, 4975.

7 a) M. Ballauff, C. N. Likos, *Angew. Chem., Int. Ed.* **2004**, *43*, 2998. b) C. J. Hawker, J. M. J. Fréchet, *J. Am. Chem. Soc.* **1992**, *114*, 8405. c) V. Maraval, R. Laurent, B. Donnadieu, M. Mauzac, A.-M. Caminade, J.-P. Majoral, *J. Am. Chem. Soc.* **2000**, *122*, 2499.

8 K. Yamamoto, M. Higuchi, S. Shiki, M. Tsuruta, H. Chiba, *Nature* **2002**, *415*, 509.

9 M. Higuchi, M. Tsuruta, H. Chiba, S. Shiki, K. Yamamoto, *J. Am. Chem. Soc.* **2003**, *125*, 9988.

10 R. Nakajima, M. Tsuruta, M. Higuchi, K. Yamamoto, *J. Am. Chem. Soc.* **2004**, *126*, 1630.

11 O. Enoki, T. Imaoka, K. Yamamoto, *Bull. Chem. Soc. Jpn.* **2006**, *79*, 621.

12 K. Yamamoto, M. Higuchi, A. Kimoto, T. Imaoka, K. Masachika, *Bull. Chem. Soc. Jpn.* **2005**, *78*, 349.

13 P. Job, *Ann. Chim.* **1928**, *9*, 113.

14 W. C. Vosburgh, G. R. Cooper, *J. Am. Chem. Soc.* **1941**, *63*, 437.

15 Z. D. Hill, P. MacCarthy, *J. Chem. Educ.* **1986**, *63*, 162.

16 Because the complexation ability of Fe and Ga in acetonitrile/chloroform was too high to compare, the experiments were performed in acetonitrile/tetrahydrofuran. Generally, the complexation ability decreases in polar solvent, so tetrahydrofuran was a good solvent for comparing the complexation ability.

17 The absorbance (Abs.) of the solution and K between metal salt and DPA imine are represented as follows; $K = C_{\text{complex}}/(C_{\text{metal}}C_{\text{imine}})$, $\text{Abs.} = \varepsilon_{\text{metal}}C_{\text{metal}} + \varepsilon_{\text{imine}}C_{\text{imine}} + \varepsilon_{\text{complex}}C_{\text{complex}}$. The replacement of C_{complex} as x gives the equations; $K = x/\{(M_0 - x)(L_0 - x)\}$, $\text{Abs.} = \varepsilon_{\text{metal}}(M_0 - x) + \varepsilon_{\text{imine}}(L_0 - x) + \varepsilon_{\text{complex}}x$, where M_0 is the concentration of the amount of the added metal salts and L_0 is the initial concentration of the imine on DPA. Curve fitting of the experimental data gave the coordination constant (K) between metal salt and imine on DPA.

18 N. Toshima, T. Yonezawa, *New J. Chem.* **1998**, *22*, 1179.

19 S. Sun, C. B. Murray, D. Weller, L. Folks, A. Moser, *Science* **2000**, *287*, 1989.

20 S. Zhou, B. Varughese, B. Eichhorn, G. Jackson, K. McIlwrath, *Angew. Chem., Int. Ed.* **2005**, *44*, 4539.

21 Calculation based on the occupied volume at 14 equivalent amounts as 2.0 nm gave us an estimate that the size of the whole dendrimer complex will be 2.5 to 2.6 nm with the molecular size being 1.95 to 2.04 nm.

22 N. N. Greenwood, T. C. Gibb, *Mössbauer Spectroscopy*, Chapman and Hall, London, U.K., **1971**.

23 a) F. Genoud, I. Kulszewicz-Bajer, A. Bedel, J. L. Oddou, C. Jeandey, A. Pron, *Chem. Mater.* **2000**, *12*, 744. b) I. Kulszewicz-Bajer, J. Suwalski, *Synth. Met.* **2000**, *12*, 744. c) V. Arora, Rajesh, P. Mathur, S. R. Vadera, *Transition Met. Chem.* **1999**, *24*, 92.

24 a) R. D. Feltham, P. Brant, *J. Am. Chem. Soc.* **1982**, *104*, 641. b) C. D. Cook, K. Y. Wan, U. Gelius, K. Hamrin, G. Johansson, E. Olsson, H. Siegbahn, C. Nordling, K. Siegbahn, *J. Am. Chem. Soc.* **1971**, *93*, 1904. c) H. Inoue, T. Kobayashi, E. Fluck, *Hyperfine Interact.*, **1994**, *68*, 193. d) M. Endo, Z. Jin, S. Kasai, H. Hasegawa, *Jpn. J. Appl. Phys.* **2002**, *41*, 2689.

25 Though ^{11}B is NMR active as well, it is not good in this case since its BF_3 complex is insensitive to a change in the environment and therefore not expected to cause a significant change in the chemical shift.

26 M. Higuchi, S. Shiki, K. Yamamoto, *Org. Lett.* **2000**, *2*, 3079.

27 K. Takanashi, H. Chiba, M. Higuchi, K. Yamamoto, *Org. Lett.* **2004**, *6*, 1709.

28 A. R. Pray, *Inorg. Synth.* **1957**, *5*, 153.

29 ΔA is the absorption at x equiv of metal normalized by the absorption of excess amount of metal salt. In case of $FeCl_3$ and $GaCl_3$, 4 equiv of metal salts is the excess amount of the metals, because the change in the UV–vis spectra was saturated. In the same way, VCl_3 is 5 equiv and $SnCl_2$ is 12 equiv.